Journal of Solid State Chemistry 233 (2016) 282–288

Contents lists available at ScienceDirect

Journal of Solid State Chemistry

journal homepage: www.elsevier.com/locate/jssc

Synthesis, crystal structure, and photocatalytical properties of $Ba_3Ta_5O_{14}N$

B. Anke [a], T. Bredow [b], J. Soldat [c,d], M. Wark [d], M. Lerch [a,*]

[a] Institut für Chemie, Technische Universität Berlin, Straße des 17. Juni 135, 10623 Berlin, Germany
[b] Mulliken Center for Theoretical Chemistry, Institut für Physikalische und Theoretische Chemie, Universität Bonn, Beringstr. 4, 53115 Bonn, Germany
[c] Lehrstuhl für Technische Chemie, Ruhr-Universität Bochum, Universitätsstr. 150, 44801 Bochum, Germany
[d] Institut für Chemie, Carl von Ossietzky Universität Oldenburg, Carl-von-Ossietzky-Str. 9-11, 26129 Oldenburg, Germany

ARTICLE INFO

Article history:
Received 16 September 2015
Received in revised form
28 October 2015
Accepted 29 October 2015
Available online 30 October 2015

Keywords:
Barium tantalum oxide
Oxide nitrides
Synthesis
Crystal structure
Quantum-chemical calculations
Photocatalysis

ABSTRACT

Light yellow $Ba_3Ta_5^{V}O_{14}N$ was successfully synthesized as phase-pure material crystallizing isostructurally to well-known mixed-valence $Ba_3Ta_4^{V}Ta^{IV}O_{15}$. The electronic structure of $Ba_3Ta_5O_{14}N$ was studied theoretically with a hybrid Hartree–Fock-DFT method. The most stable structure was obtained when nitrogen atoms were placed at 4 h sites having fourfold coordination. By incorporating nitrogen, the band gap decreases from ~3.8 eV commonly known for barium tantalum(V) oxides to 2.8 eV for the oxide nitride, giving rise to an absorption band well in the visible-light region. $Ba_3Ta_5O_{14}N$ was also tested for photocatalytic hydrogen formation.

1. Introduction

Taking a look on ternary barium tantalum oxides reported in literature, a variety of phases with different compositions is reported: $BaTa_2O_6$, [1] $Ba_2Ta_5O_{32}$, [2] $Ba_5Ta_4O_{15}$, [3] and $Ba_4Ta_2O_9$ [4] have been already described. It is worth mentioning that also two mixed-valent compounds, $Ba_{1.88}Ta_{15}O_{32}$[5] and $Ba_3Ta_5O_{15}$ [6], are known. Interestingly, remarkable photocatalytic activity (water splitting, H_2-evolution) is observed for $Ba_3Ta_4^{V}Ta^{IV}O_{15}$-containing composites [7]. $Ba_3Ta_5O_{15}$ exhibits the well-known tetragonal tungsten bronze structure (space group *P*4/*mbm* [6]) and can be described as vertex-sharing framework of TaO_6-octahedra forming huge sites where larger metal cations are located.

Photocatalytic activity under visible light ($420\ nm < \lambda < 800\ nm$) requires optical band gaps of $E_g < 2.9$ eV. Barium tantalum oxides typically have values above 3.5 eV. A common strategy to narrow the optical band gap in oxides is the partial substitution of oxygen by aliovalent anions. In 2001, Asahi et al. predicted a reduction of the band gap of titania maintaining the conduction band (CB) minimum level and shifting the valence band (VB) maximum to a position with more negative potential [8]. Their studies initiated a lot of efforts in investigating anion substitution in photocatalysts using a number of 'dopant elements' such as B [9–11], C [12–16], F [17–21], N [22–26], P [12], or S [27–30] to narrow optical band gaps to the visible-light region for various semiconductor materials. Among these, nitrogen has been reported to be the most effective dopant so far. Also several visible light-driven semiconductors containing photocatalysts including tantalum oxide nitrides are known to perform photocatalytic water splitting [31–33]. In the present contribution, we report on synthesis, crystal structure incl. N/O distribution, optical properties, and photocatalytic activity of the new compound $Ba_3Ta_5^{V}O_{14}N$ formally derived from $Ba_3Ta_4^{V}Ta^{IV}O_{15}$ by substituting one oxygen by nitrogen combined with an oxidation of Ta^{IV} to Ta^{V}. It should be mentioned that first attempts preparing such an oxide nitride phase have been carried out by Assabaa-Boultif [34] but never been published in a regular journal.

2. Experimental section

2.1. Synthesis

An amorphous ternary Ba–Ta–O phase was synthesized via the sol–gel based Pechini route [35]. Citrate complexes of tantalum and barium were prepared. For the barium citrate solution barium chloride powder (Sigma Aldrich, 99.9%) was dissolved in an ethanol/water mixture containing citric acid (Sigma Aldrich 99.5%). Citric acid was used in a molar excess of 12 times the $BaCl_2$.

* Corresponding author.

http://dx.doi.org/10.1016/j.jssc.2015.10.042
0022-4596/

Tantalum citrate solution was prepared using tantalum(V) chloride powder (Sigma Aldrich, 99.999%) by dissolving it in ethanol containing citric acid as well. Both solutions were mixed in a molar ratio of 3:5 with ethylene glycol and polymerized at 200 °C in a batch furnace. After calcination at 400 °C, an amorphous oxide was obtained. This precursor was treated with a mixture of NH_3 and O_2 at 850 °C for 24 h in a tube furnace with flow rates of 10 L h^{-1} and 0.03 L h^{-1} for ammonia and oxygen, respectively.

2.2. Chemical and structural characterization

The products were characterized by X-ray powder diffraction using a PANalytical X'Pert PRO diffractometer (Bragg–Brentano geometry, Cu-Kα radiation). All structural refinements were performed with the program *FullProf* Suite Version 2009, by applying a pseudo-Voigt function for the microstructural analysis [36]. Nitrogen and oxygen contents were determined by hot gas extraction method (LECO TC-300/EF-300), for calibration ZrO_2 and steel (LECO calibration sample, N: 5000 ppm) were used as standard materials. The accuracy is ~2% of the presented N/O content. X-ray fluorescence spectrometry (XRF) was performed using a PANalytical Axios spectrometer with an Rh-tube.

2.3. UV–vis spectroscopy

UV–vis diffuse reflectance spectra were measured using a Perkin Elmer Lambda 650 UV–vis spectrometer equipped with a Praying-Mantis mirror construction. The obtained spectra were converted by the Kubelka–Munk function $F(R)$ into absorption spectra, using MgO nanopowder as a white standard. Optical band gaps (E_g) were obtained via the Tauc plot method [30,37–41] using the calculation $\alpha = A(h\nu - E_g)^n/h\nu$, where α is the absorption coefficient, A is a constant, $h\nu$ is the energy of light, and $n=2$ is valid for materials with indirect band gap transition, respectively. Assuming the absorption coefficient α being proportional to the Kubelka-Munk function $F(R)$, E_g can be obtained from the plot of $[F(R)h\nu]^{1/n}$ versus $h\nu$, by extrapolation of the linear part near the onset of the absorption edge to intersect the energy axis.

2.4. Quantum-chemical methods

The effect of O/N distribution on the stability and electronic structure of $Ba_3Ta_5O_{14}N$ was calculated from first principles employing hybrid density functional theory (DFT) methods implemented in the crystalline-orbital program CRYSTAL14 [42]. Similar to our previous studies on TaON [43] the method PW1PW [44] was employed for the structure optimizations. For the structure optimizations standard basis sets (std) from the CRYSTAL homepage were used [45]. For the calculation of the electronic structure we employed the recently developed hybrid method HSE06 with screened exchange [46] which was demonstrated to provide improved band gaps of oxides. Since also the atomic basis set affects the band positions, we switched from standard to extended basis sets of triple-zeta valence plus polarization (tzvp) quality. For O and N, we employed the pob basis sets [47], and for Ta and Ba Stuttgart/Dresden effective core potentials plus modified triple-zeta basis sets [48,49] where diffuse functions were removed.

2.5. Photocatalysis

Photocatalytic hydrogen generation was measured in a homemade air-free closed gas system using a double-walled inner irradiation-type quartz reactor. As a light source, a 700 WHg mid-pressure immersion lamp (Peschl UV-Consulting, set to a power of 500 W) was used for irradiation and cooled with a double-walled quartz mantle using a thermostat (LAUDA). Gas evolution was detected online using a multi-channel analyzer (Emerson) equipped with a detector for the determination of the concentration of hydrogen (thermal conductivity detector), oxygen (paramagnetism) and carbon dioxide (IR). Argon was used as carrier gas, the continuous gas flow was controlled by a Brockhorst mass flow controller. The gas flow was set to 50 N mL/min (normal flow throughput: gas flow at ambient temperature and pressure per minute).

All reactions were performed at 13 °C. 300 mg of photocatalyst is suspended in 550 mL water and 50 mL methanol (aqueous methanol photoreforming). For a homogeneous suspension a subsequent pre-treatment in the ultrasonication bath for 10 min at 30 °C was performed. Before any photocatalytic reaction was initiated, the whole system including the photocatalyst was flushed with argon at 100 NmL/min for 30 minutes to remove any trace of air. In previous measurements Rh was obtained as the most effective co-catalyst for barium tantalates with an optimum loading of only 0.0125 wt%. Rh [7,50] nanoparticles were deposited onto the photocatalyst materials via reductive photodeposition with a specific amount of Na_3RhCl_6 (99.999%, Aldrich) precursor solution using the setup described below. For measurements under visible light an aqueous 2 M $NaNO_2$ solution was used as filter.

3. Results and discussion

3.1. Chemical analysis and crystal structure

We successfully synthesized light yellow $Ba_3Ta_5O_{14}N$ as phase-pure material: XRF analysis proved the Ba/Ta content of 26 wt% Ba and 58 wt% Ta (expected: 26.5 wt% Ba, 58.1 wt% Ta). Quantitative chemical analysis by hot gas extraction delivered the following values: 15.0 wt% O, 0.9 wt% N (expected: 14.4 wt% O, 0.9 wt% N).

The structural refinement of $Ba_3Ta_5O_{14}N$ was started from the coordinates reported for $Ba_3Ta_5O_{15}$ [6]. Fig. 1 depicts the X-ray powder diffractogram of the new phase $Ba_3Ta_5O_{14}N$ with the results of the Rietveld refinement. Further structural parameters are listed in Table 1 with a comparison to $Ba_3Ta_5O_{15}$. Atomic coordinates and isotropic Debye–Waller factors are presented in Table 2. For comparison, we also prepared $Ba_3Ta_5O_{15}$, following the work of Feger and Ziebarth [6]. The refined structural parameters are in good agreement. Finally, we decided to use the parameters from literature for discussion because of the higher quality of the single crystal data.

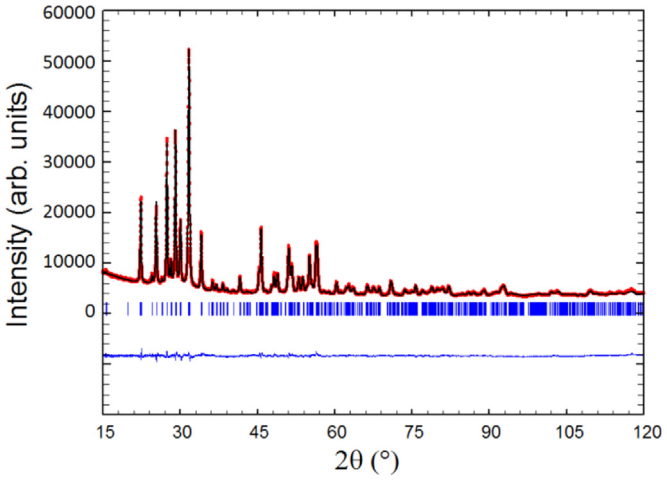

Fig. 1. X-ray powder diffraction pattern of $Ba_3Ta_5O_{14}N$ with the results of the Rietveld refinement.